

# Preparation and properties of chromium-containing hydrotreating catalysts (Ni–Mo)/ZrO<sub>2</sub>–Cr<sub>2</sub>O<sub>3</sub>

A. Thiollier, P. Afanasiev\*, M. Cattenot and M. Vrinat

*Institut de Recherches sur la Catalyse 2, avenue A. Einstein, 69626 Villeurbanne Cédex, France*

Received 6 May 1998; accepted 4 August 1998

The properties of hydrotreating catalysts (Ni–Mo)/ZrO<sub>2</sub>–Cr<sub>2</sub>O<sub>3</sub> containing either 10 or 90 mol% of Cr<sub>2</sub>O<sub>3</sub> have been studied in the model reactions of thiophene hydrodesulfurisation (HDS) and tetralin hydrogenation (HYD). Catalysts were characterized by X-ray diffraction, UV-visible spectroscopy and measurements of textural properties. It has been shown that the presence of chromium in the NiMo/ZrO<sub>2</sub> systems makes them more hydrogenating, because of the formation of chromium sulphide Cr<sub>2</sub>S<sub>3</sub>. Mixed hydrous or crystalline oxide Cr–Zr can be sulfided under mild conditions (400 °C, H<sub>2</sub>S/H<sub>2</sub>) leading to highly dispersed Cr<sub>2</sub>S<sub>3</sub> which is impossible for individual Cr<sub>2</sub>O<sub>3</sub>. Such systems are several times more active in HYD of tetralin than industrial NiMo/Al<sub>2</sub>O<sub>3</sub> reference catalyst. At the same time in the presence of chromium, the synergy of catalytic activity between Ni and Mo in the reaction of HDS of thiophene was lowered, apparently because of hindering of formation of mixed sulfide Ni–Mo–S active sites due to the stronger interaction between Ni and Cr species than that of Ni and Mo.

**Keywords:** chromium molybdenum nickel sulfides, zirconia-supported catalysts, hydrotreating

## 1. Introduction

Hydrotreating catalysts are used to upgrade petroleum feedstocks before they are treated over hydrocracking or reforming catalysts. The process of hydrotreating includes several reactions among which are hydrodesulfurisation (HDS), hydrodenitrogenation (HDN) and hydrogenation (HYD) [1–3]. The industrial hydrotreating catalysts use molybdenum oxide promoted by cobalt or nickel, supported on a high surface area oxide such as alumina.

The upcoming task of deep hydrodesulfurisation of oil fractions makes necessary processing the most refractory sulfur-containing molecules such as alkylbenzothiophenes. Under the conditions of HDS, these compounds are believed to be firstly hydrogenated and only then to lose sulfur [4,5]. Therefore, catalysts of enhanced hydrogenating activity present a potential interest. In order to develop hydrotreating catalysts with enhanced properties, other than alumina supports are being studied such as carbon, silica, zeolites, titania, zirconia [6], or other active phases as sulfides of Nb and Ru are used [7,8].

In previous works it has been shown that the Mo and Ni–Mo sulfide catalysts supported on ZrO<sub>2</sub> [9–11], TiO<sub>2</sub> [12] or CeO<sub>2</sub> [13] possess enhanced hydrogenating activity compared to their alumina supported analogs. It was suggested that partial reduction or sulfidation of the support enhances also the reducibility of the supported sulfide.

Chromium(III) oxide is thermally almost as stable as conventional oxide supports, but its surface should be more reducible than that of alumina or zirconia (since Cr(II) species are relatively stable). Therefore, mixed oxide sup-

ports containing Cr(III) should also have enhanced reducibility and/or sulfidability. For example, mixed oxides of Cr and Ti easily activate H<sub>2</sub>S, being used as electric resistivity sensors for this gas [14].

On the other hand, there have been only few studies on the properties of chromium sulfide in hydrotreating reactions. It showed moderated HYD and HDS activity per unit of surface, comparable to that of Mo and W sulfides [15], though its promotion effect with other transition group metals is unknown. The advantage of chromium sulfide might be its high thermal stability, which could allow one to obtain this sulfide in highly dispersed state, possessing good textural properties comparable to industrial catalysts.

The above considerations encouraged us to prepare chromium-containing catalysts, in order to study the eventual effect of Cr on the catalytic properties of known systems, which are (Ni)Mo/ZrO<sub>2</sub>-supported catalysts. Chromium was introduced in an oxide support in the combination with ZrO<sub>2</sub>, either as an admixture or as a main component. Of course, since chromium oxide could be transformed to sulfide in the presence of H<sub>2</sub>S it was impossible to say in advance whether the chromium from the mixed Zr–Cr oxides could be sulfided and therefore become an active sulfide phase, or remain inside the support, just modifying its properties. Moreover, there is no physico-chemical information at all on the interaction between the active phases of (Ni)Mo sulfide catalysts and chromium oxide or sulfide(s). Our goal in this work was to study the properties of these chromium-containing catalysts, otherwise similar to the (Ni)Mo/ZrO<sub>2</sub> systems which have been extensively studied in our laboratory [11,16,17].

\* To whom correspondence should be addressed.

Table 1  
Composition and textural properties of Cr-containing catalysts.

Name	Cr <sub>2</sub> O <sub>3</sub> (%)	Mo (%)	Ni (%)	S <sup>a</sup> (m <sup>2</sup> /g)	R(p) <sup>b</sup> (nm)
ZC10	10	0	0	202	1.6
ZC90	90	0	0	186	1.8–5
MZC10-773	10	9	0	239	1.8–3
MZC90-773	90	9	0	125	8
NMZC10-773	10	9	3	212	1.8–3
NMZC10-873	10	9	3	117	2.5
NMZC90-773	90	9	3	148	1.8–8
MZC90-S <sup>c</sup>	90	9	0	140	5

<sup>a</sup> The error of specific surface area measurement is  $\pm 5$  m<sup>2</sup>/g.

<sup>b</sup> R(p) is the value of maximum of pore radii distribution.

<sup>c</sup> Sulfided sample.

## 2. Experimental

### 2.1. Preparation of catalysts

First, mixed ZrO<sub>2</sub>–Cr<sub>2</sub>O<sub>3</sub> oxide supports were prepared, containing either 10 or 90 mol% of Cr<sub>2</sub>O<sub>3</sub>. The mixture of hydrated salts CrCl<sub>3</sub> and ZrOCl<sub>2</sub> was dissolved in water, then coprecipitated with aqueous ammonia up to pH 10 (at higher pH Cr begins to be redissolved by ammonia). The precipitate was washed with boiling water in a Soxhlet apparatus. The level of chloride impurity determined potentiometrically with a selective electrode was less than 300 ppm. Hydrous precipitates obtained were either calcined and used directly as catalysts, or they were impregnated with the aqueous solutions of hydrated Ni(NO<sub>3</sub>)<sub>2</sub> and (NH<sub>4</sub>)<sub>6</sub>Mo<sub>7</sub>O<sub>24</sub>. The composition of catalysts obtained is given in table 1. In this table the names of samples are composed by the first letters of the elements included in the sample followed by the number (90 for chromium-rich and 10 for zirconium-rich samples) as well as the calcination temperature at the end.

Catalysts were calcined at 773–873 K for 2 h under a nitrogen flow (to avoid oxidation of Cr to chromate, which was proved to be bad for the catalytic properties). Sulfidation was done in a glass reactor at 673 K for 4 h under a flow of 15% H<sub>2</sub>S in N<sub>2</sub> gaseous mixture.

### 2.2. Characterisations

X-ray diffraction patterns were obtained on a Siemens diffractometer with Cu K $\alpha$  emission. The diffractograms were analysed using the standard JCPDS files. UV-visible diffuse reflectance spectra were measured on a Perkin-Elmer lambda 9 spectrometer, using BaSO<sub>4</sub> as a reference. Surface area and pore volume were measured with low-temperature adsorption of nitrogen, and calculated according to BET and BJH equations.

### 2.3. Catalytic tests

Thiophene HDS and tetralin HYD reaction were chosen as model reactions for the comparison of the catalytic properties.

Thiophene HDS was carried out in the vapour phase in a fixed bed microreactor operated in the dynamic mode at the atmospheric pressure of hydrogen without addition of H<sub>2</sub>S (thiophene pressure: 2.4 kPa, total flow: 6 l/h). A catalyst charge of about 0.1 g was employed. For tetralin gas phase HYD, the experimental conditions were so chosen to avoid thermodynamic equilibrium which would favour dehydrogenation to form naphthalene. The range of temperatures studied was 523–573 K, the hydrogen pressure 4.5 MPa, the tetralin vapour partial pressure 8.9 kPa and H<sub>2</sub>S pressure 84 kPa. In all the catalytic tests, the reaction rate (specific rate) was calculated at 573 K after 16 h on stream in the pseudostationary state 16 h of stream according to the equation:

$$R = FX/m,$$

where  $R$  is the specific rate (mol/g s),  $F$  the molar flow rate of the reactant (mol/s),  $X$  is the conversion of reactant, and  $m$  is the catalyst weight (g).

In both catalytic tests the products were analysed chromatographically. The relative error of catalytic activity measurements was about 10%.

## 3. Results and discussion

### 3.1. XRD study

All the non-calcined specimens were XRD amorphous, showing in the case of Zr-rich solids broad maxima, characteristic of hydrous zirconia, and showing no peaks at all for Cr-rich ones.

After calcination under nitrogen flow at 773 K, in the zirconium-rich sample ZC10, tetragonal zirconia was detected with slightly decreased cell parameters, apparently due to the formation of a solid oxide solution (though the crystallinity of powder was not sufficient to measure it reliably, figure 1(a)). After Mo addition (MCZ10), crystallisation was more difficult, so that calcination at 823–873 K was necessary to make ZrO<sub>2</sub> lines appear in XRD patterns.

The sample containing 90% of Cr<sub>2</sub>O<sub>3</sub> (ZC90) after calcination at 500 °C crystallised as Cr<sub>2</sub>O<sub>3</sub> (JCPDS 6-0504). Addition of Mo slowed down its crystallisation again, but this time, the effect was less pronounced. Moreover, selective suppression of certain XRD reflections of Cr<sub>2</sub>O<sub>3</sub> was observed (figure 2). Apparently, it happens because molybdate has very different affinity to different crystalline planes of Cr<sub>2</sub>O<sub>3</sub> which is not the case of ZrO<sub>2</sub>, therefore it hinders growth of some planes more than others (this observation might be interesting by itself, but its study is out of the scope of this work).

Addition of Ni does not change anything in the XRD patterns, which is not surprising taking into account its low content.

The conclusions from the XRD study of oxides are simple: XRD-homogeneous solids were obtained in all cases, containing apparently solid solutions on the base of the

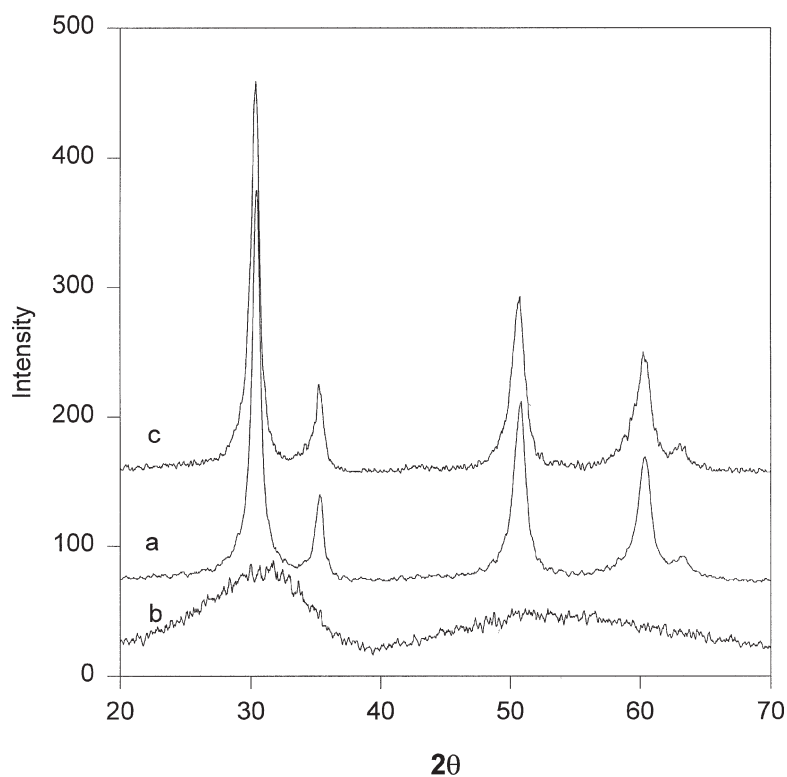


Figure 1. X-ray diffraction patterns of samples CZ10-773 (a), MCZ10-773 (b) and CZ10-873 (c). All peaks – tetragonal zirconia (JCPDS 27-0997).

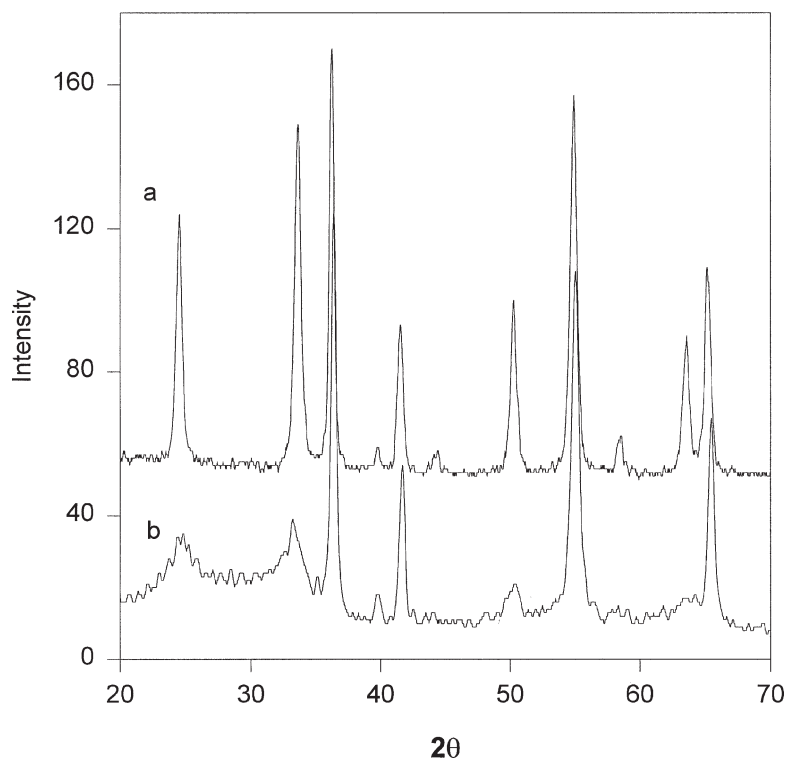


Figure 2. X-ray diffraction patterns of samples CZ90-773 (a) and MCZ90-773 (b). All peaks –  $\text{Cr}_2\text{O}_3$  (JCPDS 38-1479).

corresponding main composing oxides. Addition of Mo hinders crystallisation during calcination both of zirconium and chromium oxides, but this effect was more pronounced for Zr-rich solids.

Sulfidation of chromium-rich solids ( $xx\text{ZrC}90-y$ ) at 673 K leads to the formation of dispersed  $\text{Cr}_2\text{S}_3$  sulfide (figure 3(a)), whereas this phase cannot be prepared under the same conditions from  $\text{Cr}_2\text{O}_3$ , either the hydrous oxide

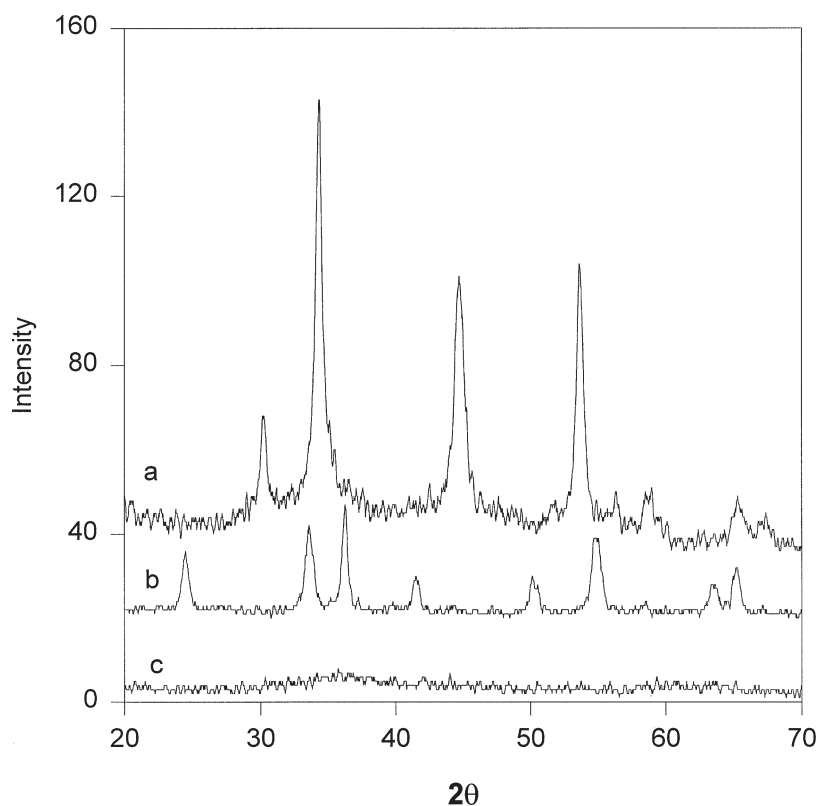


Figure 3. X-ray diffraction patterns of samples sulfided at 673 K: CZ90 (a), all peaks –  $\text{Cr}_2\text{S}_3$  (JCPDS 10-0340);  $\text{Cr}_2\text{O}_3$  (b), all peaks –  $\text{Cr}_2\text{O}_3$  (JCPDS 38-1479); and dried hydrous chromium oxide (c).

freshly precipitated from  $\text{CrCl}_3$  solution with ammonia or the crystallised oxide obtained by calcination of the above mentioned precipitate at 773 K for 2 h (figure 3 (b), (c)). The same observation concerning the difficulty of sulfiding of  $\text{Cr}_2\text{O}_3$  was made earlier by Sukhareva et al. [18]. To obtain chromium sulfide, sulfidation of chloride [15] or precipitation of sulfide from non-aqueous solvents [19] was applied. Therefore, in the ZC90 samples the presence of some zirconium makes sulfidation of  $\text{Cr}_2\text{O}_3$  much easier so that complete transformation to  $\text{Cr}_2\text{S}_3$  becomes possible under the conditions used.

Zirconium-rich specimens  $xx\text{ZC}10-y$  do not show any new phases after sulfidation.

### 3.2. Textural properties

The textural properties of solids are listed in table 1. It can be seen that the addition of Mo stabilises the surface areas of zirconia-supported catalysts, as discussed previously for (Ni)Mo/ZrO<sub>2</sub> catalysts [16,20,21]. Zirconium-rich samples show surface areas and porosity close to those observed earlier for the solids prepared under the same conditions, but without addition of Cr. Chromium-rich samples showed somewhat lower surface areas, but much higher pore sizes, lying completely in the domain of mesoporosity.

It should be emphasised that hindering of crystallisation and stabilisation of surface area by molybdate species have quite independent physical nature: the former is a purely kinetic effect whereas the latter is related to the formation

Table 2  
Catalytic activity in the model HDS and HYD reactions, measured at 573 K.

Name	$A(\text{HYD}) \times 10^{-8}$ (mol/g s)	$A(\text{HDS}) \times 10^{-8}$ (mol/g s)
ZC10	3	11
ZC90	41	47
MZC10-773	18	38
MZC90-773	52	54
NMZC10-773	19	36
NMZC10-873	11	107
NMZC90-773	43	70
Mo/ZrO <sub>2</sub>	16	24
NiMo/ZrO <sub>2</sub>	27	140
Mo/Al <sub>2</sub> O <sub>3</sub>	4	12
NiMo/Al <sub>2</sub> O <sub>3</sub>	14	160

of a thermodynamically metastable state [21]. Therefore, even well crystallised catalysts can undergo a stabilising effect of the supported Mo oxospecies as described in [20].

### 3.3. Catalytic properties

Steady-state catalytic activities estimates as the rates of the HYD and HDS model reactions measured at 573 K are listed in table 2. For comparison, the activities measured at the same conditions for an impregnated Mo/Al<sub>2</sub>O<sub>3</sub>, an industrial reference NiMo/Al<sub>2</sub>O<sub>3</sub>, and for Mo/ZrO<sub>2</sub> and NiMo/ZrO<sub>2</sub> catalysts, prepared by the same method, and containing the same amount of Ni and Mo, are reported.

Though we do not discuss in this paper the samples obtained using calcination in air, it might be worth noting that all those systems contained considerable amounts of chromate, and showed low activity, compared to those of non-calcined or calcined under nitrogen flow systems of the same composition. Only the latter are considered here.

It can be seen from table 2 that the HYD activity of chromium-containing samples is in some cases several times higher than that of the NiMo/Al<sub>2</sub>O<sub>3</sub> industrial catalyst. At the same time, thiophene HDS activities are always somewhat lower than that of the industrial NiMo/Al<sub>2</sub>O<sub>3</sub> reference.

The catalysts containing chromium alone (ZC10, ZC90), initially designed as “supports”, appeared to be active in both the HYD and HDS reactions. The catalyst containing 10% of Cr was as active as a non-promoted Mo/alumina reference system. The chromium-rich sample ZC90 showed, as can be expected, a much higher activity, though no direct proportionality to Cr content was found, neither was the HYD activity in step with HDS. The activity observed is obviously due to the presence of Cr<sub>2</sub>S<sub>3</sub> formed during the sulfidation step, which was seen by XRD for the ZC90-S sample. In the case of ZC10, no direct evidence of formation of chromium sulfide was obtained, but it seems quite probable. Pure zirconia had a negligible activity in both reactions.

It seems that after sulfidation at 673 K Cr<sub>2</sub>S<sub>3</sub> can be obtained from dispersed crystalline Cr<sub>2</sub>O<sub>3</sub>–ZrO<sub>2</sub> mixed oxide or from the same hydrous oxide, prepared by precipitation and drying, but not from the solid solution of Cr(III) distributed in the ZrO<sub>2</sub> lattice, formed as a result of calcination. Indeed, crystalline sample CZ10-873 obtained from the calcination of CZ10 at 873 K was totally inactive (not shown).

The addition of Mo systematically increased the catalytic activity (samples MCZ10-773 and MCZ90-773). The HYD activity of MoZC10-773 ( $18 \times 10^{-8}$  mol/g s) was close to the sum of activities of Cr alone and Mo alone supported on zirconia ( $19 \times 10^{-8}$  mol/g s). The same was observed for the HDS activity, the corresponding values being  $38 \times 10^{-8}$  and  $35 \times 10^{-8}$  mol/g s. Therefore, in the Mo–Cr samples with low content of chromium, sulfides of Mo and Cr work together more or less independently. No promotion or poisoning was noted. The additivity of catalytic properties was very good, taking into account usual reproducibility of catalytic properties which even for the same preparation may vary by ca. 10%. This additivity is lost when we proceed to the Cr-rich samples (MCZ90-773): catalytic activity in both reactions was slightly lower for the mixed Mo–Cr sample than the sum of the corresponding zirconia-supported Mo and Cr sulfide catalysts. However, this difference (52 and 57 for HYD; 54 and 71 for HDS) was low enough to suggest that just a simple steric hindrance in the mixture of dispersed sulfides is the cause of this effect.

In any case, all Cr-rich samples are strongly hydrogenating catalysts, several times more active than the industrial NiMo/Al<sub>2</sub>O<sub>3</sub> reference. Moreover, they possess enhanced surface areas and well developed large pores, quite appropriate for the eventual catalytic applications.

The situation was drastically changed for the Ni–Cr–Mo–Zr systems. Addition of Ni did not substantially increase the catalytic activity of these systems in any reaction. HYD activity of MZC10-773 and NMZC10-773 was approximately the same, whereas that of NMZC90-773 was even lower than that of the corresponding “non-promoted” MZC90-773. A similar effect of the absence of any significant effect was observed in the thiophene HDS reaction. This is in striking contrast with the properties of Mo and NiMo catalysts without chromium, listed in the same table 2, where the strong promoting effect of Ni was observed in both reactions. The activities observed for Cr-containing samples lead us to the conclusion that the presence of Cr hinders in some way the formation of this Ni–Mo–S phase, apparently because of more strong interaction between Ni and Cr than between Mo and Cr.

### 3.4. UV-visible spectra

Qualitative comparison of the corresponding UV-visible DR spectra shows that Ni–Cr interaction rather than the Ni–Mo one exists in the oxide precursors calcined at 773 K.

In the spectra of binary Mo–Zr, Cr–Zr and Ni–Zr oxide systems, the main features are the bands of charge transfer of the supported molybdates (250–300 nm, figure 4(a)), and d–d transitions of Ni(II) (230, 420 nm, figure 4(b)) and Cr(III) (250, 378 and 619 nm, figure 4(c)) and cations in the oxygen environment.

DR UV-visible spectra of Ni–Mo/ZrO<sub>2</sub> catalysts have been discussed in [16]. The effect of Ni–Mo interaction is a strong decrease (virtual disappearance) of the Ni(II) d–d bands at wavelengths above 500 nm, as well as some broadening of the charge transfer band, related to formation of superficial NiMoO<sub>4</sub> species, where Ni(II) is weakly absorbing.

In the Mo–Cr (10% Cr) supported on zirconia, the decrease of intensity of Cr(III) d–d transition (at 378 nm, figure 5(a)) was also observed, which can be attributed to the formation of more covalent environment of Cr due to bonding to molybdate, similarly to the Ni–Mo case.

By contrast, the Ni–Cr on zirconia catalyst shows a strong increase of the bands intensity in the d–d region (380 nm, figure 5(b)), probably because of some intervalent exchange Ni(II) + Cr(III)  $\rightleftharpoons$  Ni(III) + Cr(II). The coloration of mixed catalyst (black) was considerably more intense than those of Ni alone (light yellow) and Cr alone (light green).

Finally, the Ni–Cr–Mo on zirconia catalyst (figure 5(c)) was also black and demonstrated the same DR trend as the Ni–Cr system. Since from the above discussed spectra we know that the interactions between all three species do exist, and we know also their influence on the corresponding band intensities, we can suggest that the DR spectrum for Ni–Cr–Mo corresponds to the Ni–Cr interaction rather than to the Ni–Mo one. Indeed, if Ni(II) interacted stronger with Mo than with Cr, we would see the decrease of the band

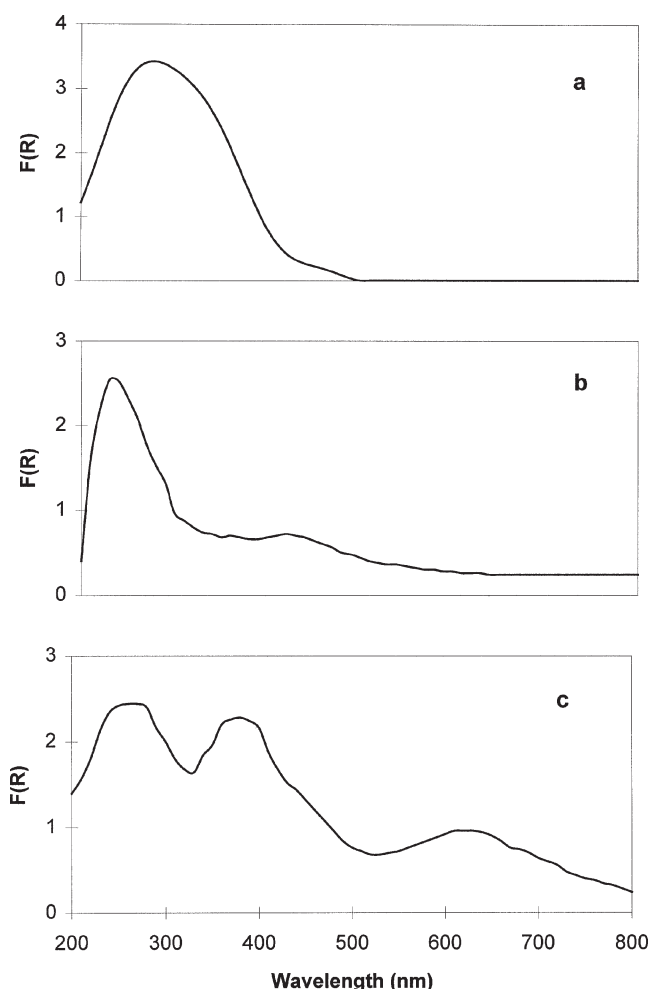


Figure 4. DR UV-visible spectra of MoO<sub>3</sub>/ZrO<sub>2</sub> (9% Mo, (a)); NiO/ZrO<sub>2</sub> (3% Ni, (b)) and sample CZ10 (c).

intensity for the Ni–Cr–Mo spectrum compared to Cr–Mo, which is not the case.

To support the qualitative speculations above, table 3, containing the absorption peak areas at 380 nm ( $^4A_{2g} \rightarrow ^4T_{2g}$  transition in the octahedral  $d^3$  ion), for different samples, might be helpful. The peak areas were calculated using the analysis of DR spectra curves by means of the PEAKFIT utility (Jandel Inc.). In fact, in the NMCZ10 catalyst, which was obtained by adding some Ni to MCZ10, the intensity of the absorption peak was the highest, suggesting Ni–Cr interaction.

With this respect it might be worth commenting on the difference between NMZC10-773 and NMZC10-873 specimens. The former is amorphous both in the oxide and the sulfide state and for a Ni–Mo catalyst possesses relatively poor HDS and moderated HYD activity. Then, when the supported Zr–Cr oxide is calcined at 600 °C, prior to impregnation with Ni and Mo, crystallisation of the Zr–Cr solid oxide solution occurs, which decreases the negative influence of Cr on the Ni–Mo promotion. Indeed, we see some increase in HDS activity due to this partially saved Ni–Mo–S phase. But at the same time, the HYD activity drops from  $19 \times 10^{-8}$  to  $11 \times 10^{-8}$  mol/g s or by ca. 40%

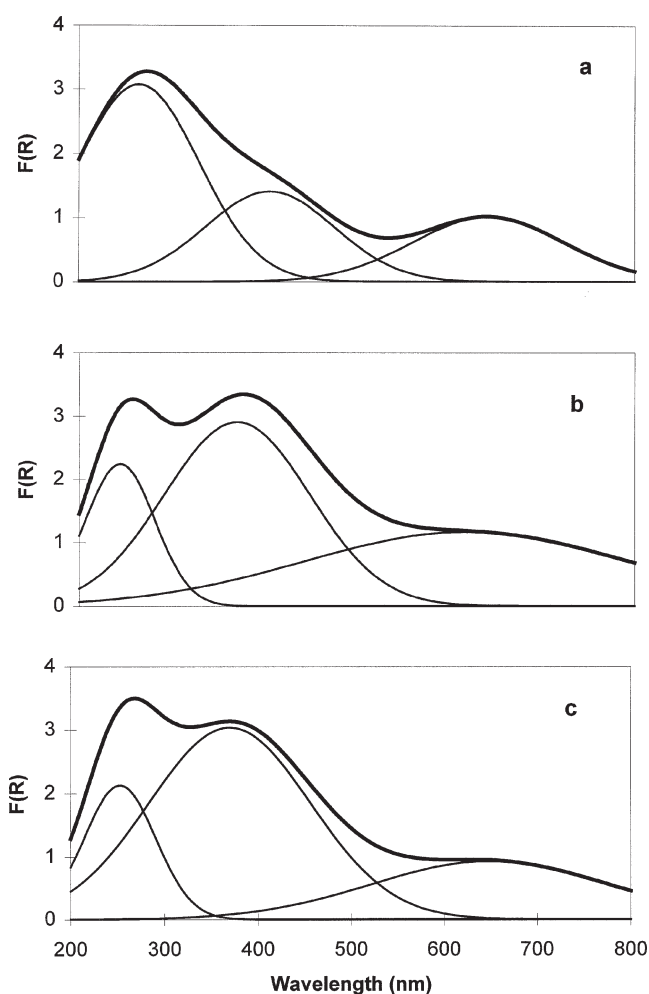


Figure 5. DR UV-visible spectra of samples MCZ10 (a), NCZ10 (b) and NMZC10 (c). Bell curves under the spectra – results of fitting with PEAKFIT utility.

Table 3  
Relative integrated intensity of the  $^4A_{2g} \rightarrow ^4T_{2g}$  transition in the UV-visible spectra of Cr-containing catalysts.

Catalyst	ZC10	NZC10	MZC10	NMZC10
I (380 nm)	485	570	344	640

of its initial value, since there is no more chromium sulfide formed.

Of course, we cannot go too far in the interpretation of these data, as concerns the nature of species formed, but the evidence of a strong Cr–Ni interaction in the Ni–Cr–Mo sample seems clear. Apparently the (CrNi)+Mo rather than Cr + (NiMo) interaction persists further in the sulfide state. At least, that is what we must conclude from the catalytic properties of solids reported here.

It should be noted that the effect reported fits to a general trend, according to which, if easier reducibility (sulfidability) of a support oxide increases the catalytic activity of unpromoted Mo sulfide supported on it, at the same time it decreases the promotion effect in the corresponding Ni–Mo supported system. Indeed, as follows from our experience

and analysis of literature works, the HYD and HDS activities of supported MoS<sub>2</sub> changes in the sequence of supports as Cr<sub>2</sub>O<sub>3</sub>, CeO<sub>2</sub> > TiO<sub>2</sub> > ZrO<sub>2</sub> > Al<sub>2</sub>O<sub>3</sub>. At the same time, the promoting effect of Ni as well as the absolute values of the activity of the corresponding Ni–Mo catalysts decrease in the inverted row: Al<sub>2</sub>O<sub>3</sub> > ZrO<sub>2</sub> > TiO<sub>2</sub> > Cr<sub>2</sub>O<sub>3</sub>, CeO<sub>2</sub>. The last two oxides present a limiting case when sulfidation is total, leading to the formation of crystalline sulfides which may have their own activity, whereas titania and zirconia do not form sulfide phases but are only superficially modified, and alumina seems not to undergo any significant transformations at all.

## References

- [1] H. Topsøe, B.C. Clausen and F.E. Massoth, *Hydrotreating Catalysis, Science and Technology* (Springer, Berlin, 1996).
- [2] G.C. Shuit and B.C. Gates, *AIChE J.* 19 (1973) 417.
- [3] F.E. Massoth, *Adv. Catal.* 27 (1978) 265.
- [4] V. Lamure-Meille, E. Shulz, M. Lemaire and M. Vrinat, *J. Catal.* 170 (1997) 29.
- [5] M.V. Landau, D. Berger and M. Herskovitz, *J. Catal.* 158 (1996) 236.
- [6] M. Breyse, J.L. Portefaix and M. Vrinat, *Catal. Today* 10 (1991) 489.
- [7] C. Geantet, J. Afonso, M. Breyse, N. Allali and M. Danot, *Catal. Today* 28 (1996) 23.
- [8] A. de Los Reyes, M. Vrinat, C. Geantet and M. Breyse, *Catal. Today* 10 (1991) 645.
- [9] J.C. Duchet, M.J. Tillette, D. Cornet, L. Vivier, G. Perot, L. Bekakra, C. Moreau and G. Szabo, *Catal. Today* 10 (1991) 579.
- [10] F. Mauge, J.C. Duchet, J.C. Lavalley, S. Housseny, E. Payen, J. Grimblot and S. Kasztelan, *Catal. Today* 10 (1991) 561.
- [11] D. Hamon, M. Vrinat, M. Breyse, B. Durand, M. Jebrouni, M. Roubin, P. Magnoux and T. des Courieres, *Catal. Today* 10 (1991) 613.
- [12] J. Ramirez, L. Ruiz-Ramirez, V. Harle, M. Vrinat and M. Breyse, *Appl. Catal. A* 93 (1993) 163.
- [13] C. Mauchaussé, H. Mozzanega, P. Turlier and J.A. Dalmon, in: *Proceedings 9th International Congress on Catalysis*, Vol. 2, eds. M.J. Phillips and M. Ternan, Calgary, 1988 (Chem. Inst. of Canada, Ottawa, 1988) p. 775.
- [14] G.S. Henshaw, D.H. Dawson and D.E. Williams, *J. Mater. Chem.* 5 (1995) 1791.
- [15] M. Lacroix, N. Boutarfa, C. Guillard, M. Vrinat and M. Breyse, *J. Catal.* 120 (1989) 473.
- [16] P. Afanasiev, C. Geantet, M. Breyse and T. des Courieres, in: *Hydrotreating Technology for Pollution Control*, eds. M.L. Occelli and R. Chianelli (Dekker, New York, 1996) p. 235.
- [17] P. Afanasiev, C. Geantet and M. Breyse, *J. Catal.* 153 (1995) 17.
- [18] T.S. Sukhareva, L.V. Shchepel and A.V. Mashkina, *Kinet. Katal.* 19 (1978) 654.
- [19] T.A. Pecoraro and R.R. Chianelli, *J. Catal.* 67 (1981) 430.
- [20] P. Afanasiev, C. Geantet and M. Breyse, *J. Mater. Chem.* 4 (1994) 1653.
- [21] P. Afanasiev, *Mater. Chem. Phys.* 47 (1997) 231.